ELSEVIER

Journal of Alloys and Compounds 356–357 (2003) 91–95

Journal of ALLOYS AND COMPOUNDS

www.elsevier.com/locate/jallcom

$Zr_4Al_3D_{2.68}$ and $Zr_3Al_2D_{2.26}$: new Zr-containing intermetallic hydrides with ordered hydrogen sublattice

A.B. Riabov[a], V.A. Yartys[b,*], R.V. Denys[a], B.C. Hauback[b]

[a]*Physico-Mechanical Institute of the National Academy of Sciences of Ukraine, 5 Naukova Street, 79601 Lviv, Ukraine*
[b]*Institute for Energy Technology, P.O. Box 40, Kjeller N-2027, Norway*

Received 11 July 2002; accepted 26 October 2002

Abstract

Two hydrogenated intermetallics with the highest Al/Zr ratio among the hydrogen-absorbing Zr–Al compounds, Zr_4Al_3 and Zr_3Al_2, have been studied by synchrotron X-ray, powder neutron diffraction and thermal desorption spectroscopy. Initial intermetallic compounds are quite different with respect to Al–Al interactions and contain plain Kagome Al nets (Zr_4Al_3) or Al–Al pairs (Zr_3Al_2). In hexagonal $Zr_4Al_3D_{2.68}$ (space group (s.g.) $P6_322$; $a=11.0017(4)$; $c=11.1694(5)$ Å) a $2a\times2a\times2c$ superstructure is formed as a result of deuterium ordering in half of the available Zr_4 tetrahedra. These tetrahedra share common corners and edges and form layers separated by 6363 Al-nets. In tetragonal $Zr_3Al_2D_{2.26}$ (s.g. $P4_2/mnm$; $a=7.5970(3)$; $c=7.2613(3)$ Å) in addition to the completely filled Zr_4 tetrahedra hydrogen partially occupies Zr_3 triangular sites. Thermal stability of the studied deuterides and Zr–D bonding characteristics can be related to the size of the occupied Zr_4 tetrahedra. Higher thermal stability of $Zr_3Al_2D_{2.26}$ agrees well with the existence of large Zr_4 sites and contrasts to the behavior of $Zr_4Al_3D_{2.68}$ containing 'contracted' Zr_4 tetrahedra and having weaker Zr–D bonds.

Keywords: Hydrogen storage materials; Gas–solid reactions; Neutron diffraction; X-ray synchrotron diffraction; Crystal structure and symmetry

1. Introduction

Hydrogen storage capacities of binary Zr–Al intermetallic compounds strongly depend on the relative Zr content in the alloys. The highest values, 0.9–1.0 at.H/M, are reached in $Zr_2AlH_{2.7}$ [1] and $Zr_5Al_3H_{8.0}$ [2] (62.5–66.7 at.% Zr). Following a decrease of Zr content in the intermetallics to 57.1–60.0 at.% Zr, the hydrogenation capacities drop significantly, to 0.5 at.H/M in $Zr_3Al_2H_{2.5}$ [1] and $Zr_4Al_3H_{3.7}$ [3].

Despite the detailed data concerning the hydrogenation properties of a few Zr–Al compounds are available, the crystal structure data are published only for one deuteride, oxygen-stabilised $Zr_5Al_3O_{0.5}D_{2.7}$ [4].

This work is aimed on studying by means of powder neutron and X-ray diffraction the crystal structures of two new compounds, $Zr_4Al_3D_{2.68}$ and $Zr_3Al_2D_{2.26}$.

2. Experimental

The alloys, Zr_4Al_3 and Zr_3Al_2, were prepared by argon arc melting of the stoichiometric mixtures of high purity constituent elements, Zr and Al. They were annealed in the evacuated quartz tubes at 900 °C for 7 days (Zr_4Al_3) and at 1100 °C for 48 h (Zr_3Al_2), and quenched into the ice water after the annealing. X-ray diffraction study of the prepared alloys (Siemens D 5000 diffractometer; Cu $K\alpha_1$ radiation; Bregg Brentano geometry; PSD) showed that intermetallic compounds Zr_4Al_3 and Zr_3Al_2 were formed as the main constituents of the 4:3 and 3:2 alloys, respectively. The Zr_4Al_3 alloy also contained minor additions of two secondary phases, Zr_3Al_2 and ZrAl. The Zr_3Al_2 alloy contained two admixtural intermetallics, Zr_4Al_3 and Zr_5Al_3. The refined unit cell parameters of Zr_4Al_3 (hexagonal; $a=5.424(1)$; $c=5.387(2)$ Å), Zr_3Al_2 (tetragonal; $a=7.628(1)$; $c=6.986$ (2) Å), ZrAl (orthorhombic; $a=3.434(3)$; $b=10.96(1)$; $c=4.305(5)$ Å) and Zr_5Al_3 (hexagonal; $a=8.181(3)$; $c=5.682(5)$ Å) agree well with the reference data in Ref. [5].

The prepared alloys were deuterated by charging with

*Corresponding author. Tel.: +47-63-806-453; fax: +47-64-810-920.
E-mail address: volodymyr.yartys@ife.no (V.A. Yartys).

0925-8388/02/$ – see front matter
doi:10.1016/S0925-8388(02)01217-3

deuterium (purity 99.8%) at pressures of 1–5 bar and at room temperature, after preliminary activation in secondary vacuum at 400 °C.

Structures of deuterides were refined by Rietveld-type analysis (General Structure Analysis System software (GSAS) [6]) of powder neutron diffraction data collected at PUS diffractometer on JEEP II reactor (Kjeller) (λ = 1.5555 Å; focusing Ge(511) monochromator; $2\Theta = 10$–$130°$; $\Delta 2\Theta = 0.05°$; 2400 data points). Samples were put into the sealed under argon cylindric vanadium sample cans with inner diameter 5 mm. Nuclear scattering lengths were taken from the GSAS library ($b_{Zr} = 7.16$, $b_{Al} = 3.45$, $b_D = 6.67$ fm). Since the deuterides $Zr_3Al_2D_{2.21}$ and $Zr_4Al_3D_{2.7}$ were present in both studied materials, their structures were refined step by step, in several iterations. Two other constituents of the deuterated materials, $Zr_5Al_3O_xD_{2.7}$ and ZrAl, were introduced into the refinements based on the available reference data [4,5].

Synchrotron XRD data were collected at ESRF, SNBL using monochromatic X-rays ($\lambda = 0.49868$ Å) obtained from Si(111). The samples were kept in rotating 0.3 mm sealed glass capillaries.

Model of hard spheres has been used in the calculations of the radii of interstitial sites in the structures of intermetallic compounds with the values of the radii, r_{Zr} = 1.602 Å and $r_{Al} = 1.432$ Å, taken from Ref. [7]. Crystal structure analysis was performed with use of ATOMS, Shape Software.

Thermal stability of hydrides was studied by monitoring pressure changes during their heating in secondary vacuum with a rate 2 °C/min.

3. Results and discussion

3.1. Crystal chemical analysis of intermetallic matrices as potential H storage materials

Hexagonal crystal structure of Zr_4Al_3 (own type of structure) is closely related to the $CaCu_5$-type. It can be obtained from $CaCu_5$ via substitutions 1Ca→2Zr; 2Cu(2*c*)→2Zr; 3Cu(3*g*)→3Al, changing the stoichiometry from RT_5 to R_4T_3. An important feature of the $CaCu_5$ type structure, presence of the 6363 Kagome nets, is retained in the Zr_4Al_3 structure (Al nets). In turn, Zr atoms form 6_3 nets built from the regular Zr_6 hexagons. The linear Zr chains centre these hexagons leading to a formation of the Zr_4 tetrahedra combined into the clusters of 6. The tetrahedra in a cluster are connected by sides and have one common 'axis' edge. As a result, the structure of Zr_4Al_3 can be described as an alternation along [001] of the layers of the clustered Zr_4 tetrahedra and Kagome nets of Al atoms (Fig. 1).

There are five types of tetrahedral interstices in the Zr_4Al_3 structure, including Zr_4, Zr_3Al, Zr_2Al_2 (two) and $ZrAl_3$ (Table 1). The most favourable for H insertion from chemical surrounding and size considerations are Zr_4 sites 6*j*.

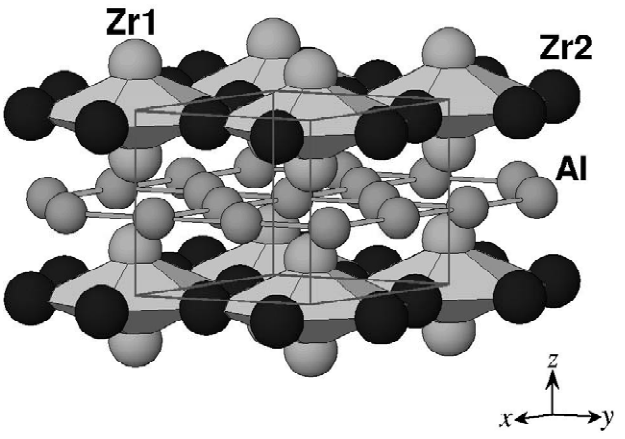

Fig. 1. The crystal structure of Zr_4Al_3. Altering layers of Zr_4 tetrahedra and plain 6363 Kagome Al-nets are shown.

Similar to Zr_4Al_3, the tetragonal crystal structure of Zr_3Al_2 is characterised by a separation of Zr and Al atoms in the structure. Zr atoms form centred cubes $ZrZr_8$, which stack into columns aligned along [001]. Via sharing the edges, the columns form a spatial network. Aluminium atoms centring the Zr_6 trigonal prisms form Al–Al pairs located inside the channels of the framework of Zr-columns.

A large number of interstices in the structure of the tetragonal Zr_3Al_2 compound includes tetrahedra Zr_4, Zr_3Al (four types) and Zr_2Al_2 and, also, two types of octahedral sites, Zr_4Al_2 and Zr_2Al_4 (Table 2). Similar to Zr_4Al_3, preferable for H insertion are Zr_4 sites ($8i_1$).

3.2. Crystal structure of $Zr_4Al_3D_{2.68}$

The synchrotron X-ray diffraction data from $Zr_4Al_3D_{2.68}$ showed that hydrogen absorption leads to the expansion of the unit cell of the compound by 6%, with no changes in the original symmetry, $\Delta a/a = 1.23\%$, $\Delta c/c = 3.46\%$. Analysis of the collected PND data indicated that deuterium atoms fill tetrahedral Zr_4 sites. It also showed an appearance of extra rather strong diffraction peaks, which

Table 1
Interstitial sites in the crystal structure of Zr_4Al_3 intermetallic compound[a]

Site	Surrounding	*x*	*y*	*z*	*r* (Å)	Neighbours
6*j*	$Zr1_2Zr2_2$	0.272	0	0	0.40	2×6*j*; 2×12*n*
12*n*	$Zr1Zr2_2Al$	0.365	0	0.188	0.40	6*j*; 12*n*; 2×12*o*
12*o*	$Zr1Zr2Al_2$	0.208	2*x*	0.293	0.37	2×12*n*; 6*m*; 4*h*
6*m*	$Zr1_2Al_2$	0.139	2*x*	1/2	0.28	2×12*o*; 2×6*m*
4*h*	$Zr2Al_3$	1/3	2/3	0.356	0.32	3×12*o*; 4*h*

Space group *P*6/*mmm* (No. 191); $a = 5.4273$; $c = 5.3927$ Å; 2 Zr1 in 2*e*: 0, 0, z, z = 1/4; 2 Zr2 in 2*c*: 1/3, 2/3, 0; 3 Al in 3*g*: 1/2, 0, 1/2.

[a] In Tables 1 and 2 the sequence of interstitial sites follows a decrease of Zr content (increase of Al content) and, for the sites with an equal surrounding, a decrease in their radii.

Table 2
Interstitial sites in the crystal structure of Zr_3Al_2 intermetallic compound

Site	Surrounding	x	y	z	r_{INT}	Neighbours
Tetrahedral interstices						
$8i_1$	$Zr1_2Zr2Zr3$	0.146	0.533	0	0.49	$2\times16k_1$; $2\times8i_2$
$8j_1$	$Zr2_2Zr3Al$	0.112	0.112	0.478	0.45	$8j_1$; $4e$; $2\times16k_1$
$16k_1$	$Zr1Zr2Zr3Al$	0.220	0.557	0.105	0.41	$8i_1$; $8j_1$; $16k_3$; $16k_2$
$16k_2$	$Zr1Zr2Zr3Al$	0.250	0.422	0.253	0.40	$16k_1$; $8j_2$; $16k_3$; $8i_2$
$16k_3$	$Zr1Zr2Zr3Al$	0.157	0.707	0.261	0.38	$16k_2$; $16k_3$; $16k_1$; $8i_2$
$8j_2$	$Zr2Zr3Al_2$	0.394	0.394	0.235	0.32	$2\times16k_2$; $4e$; $2a$
$4e$	$Zr2_2Al_2$	0	0	0.368	0.29	$2\times8j_1$; $2\times8j_2$
Octahedral interstices						
$8i_2$	$Zr1_2Zr2Zr3Al_2$	0.315	0.060	0	0.61	$2\times8i_1$; $2\times16k_2$; $2a$; $8i_2$; $2\times16k_3$
$2a$	$Zr3_2Al_4$	0	0	0	0.53	$4\times8i_2$; $4\times8j_2$

Space group $P4_2/mnm$ (No. 136); $a=7.6244$; $c=6.9862$ Å; 4 Zr1 in 4*d*: 0, 1/2, 1/4; 4 Zr2 in 4*f*: 0.34685, *x*, 0; 4 Zr3 in 4*g*: 0.19807, $-x$, 0; 8 Al in 8*j*: 0.1222, *x*, 0.2091.

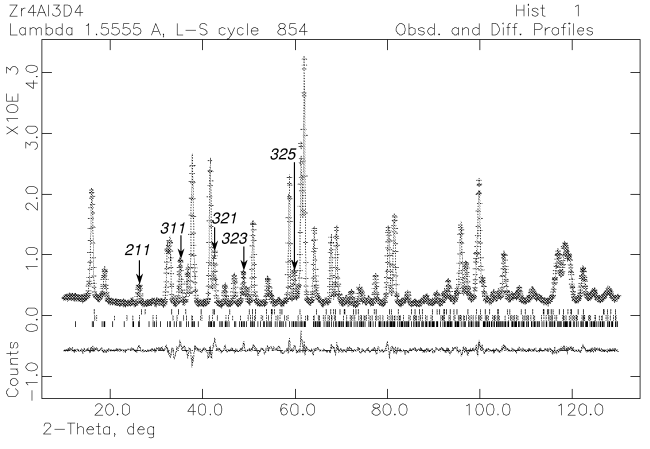

Fig. 2. PND pattern of $Zr_4Al_3D_{2.68}$ at 293 K showing observed (+), calculated (−) and difference (line at bottom) plots. The positions of the peaks of the constituent phases are marked (from bottom to top): $Zr_4Al_3D_{2.68}$, $Zr_3Al_2D_{2.26}$ and ZrAl. The Bragg indexes are given for the strongest observed superstructure peaks only (marked by arrows).

were indexed on the basis of the formation of a $2a\times2a\times2c$ superstructure. Since these peaks are not present in the XRD data, they originate from deuterium ordering (Fig. 2).

From group–subgroup relations and observed extinctions, the space group of symmetry of the formed superstructure was defined as $P6_322$ (see Table 3). In total, the supercell contains 48 Zr_4 sites. Deuterium ordering proceeds via occupation of half of the available Zr_4 tetrahedra (24). Hydrogen ordering within the Zr_4 sites proceeds in a way that neighbouring side-connected interstices are never simultaneously occupied. The doubling of the hexagonal unit cell parameters takes place due to the alternation of the occupancy of the Zr_4 sites in the hexagonal clusters of $6\times Zr_4$ (Fig. 3a, b). Furthermore, the doubling of the *c*-axis is caused by the alternation of occupancy/vacancy of the equivalent interstices aligned in the columns of these clusters.

H sublattice is built from the planar D nets separated along [001] by Al-formed Kagome nets. Thus, in

Table 3
Atomic coordinates, occupancies and temperature factors for $Zr_4Al_3D_{2.68}$ and $Zr_3Al_2D_{2.26}$ from the refinements of the PND data

	$Zr_4Al_3D_{2.68}$		$Zr_3Al_2D_{2.26}$	
Space group	$P6_322$ (No. 182)		$P4_2/mnm$ (No. 136)	
Unit cell parameters, Å	$a=11.0017(4)$ Å; $c=11.1694(5)$ Å		$a=7.5970(3)$ Å; $c=7.2613(3)$ Å	
Atomic coordinates, occupancies and temperature factors		$U_{ISO}\times100$ Å^2		$U_{ISO}\times100$ Å^2
	4 Zr1 in 4*e*: 0, 0, 0.1148(9);	1.1(3)	4 Zr1 in 4*d*: 0, 1/2, 1/4	0.33(7)
	12 Zr2 in 12*i*: 0.4966(7), 0.001(1), 0.1256(3);	0.19(9)	4 Zr2 in 4*f*: 0.3465(3), 0, 0;	0.32(7)
	4 Zr3 in 4*f*: 1/3, 2/3, 0.019(4);	0.7(4)	4 Zr3 in 4*g*: 0.1969(3), $-x$, 0;	0.30(9)
	12 Zr4 in 12*i*: 0.179(1), 0.339(3), 0.007(3);	1.0(2)	8 Al in 8*j*: 0.1226(4), *x*, 0.2103(5);	0.60(9)
	6 Al1 in 6*h*: 0.257(5), $-x$, 1/4	1.5(7)	8.00(−) D1 in 8*i*: 0.1379(3), 0.5329(3), 0;	1.02(6)
	6 Al2 in 6*h*: 0.758(5), $-x$, 1/4	3.0(9)	1.02(5) D2 in 16*k*: 0.235(3), 0.389(3), 0.274(4);	0.2(7)
	12 Al3 in 12*i*: 0.007(7), 0.249(6), 0.259(2);	1.1(3)		
	6.00(−) D1 in 6*g*: 0.144(2), 0, 0;	1.5(1)		
	4.85(10) D2 in 6*g*: 0.360(2), 0, 0;	1.6(5)		
	10.60(10) D3 in 12*i*: 0.366(2), 0.511(2), 0.001(3);	2.7(3)		
R_{pr}	5.86		4.28	
R_{wpr}	7.86		5.41	
χ^2	2.662		1.192	

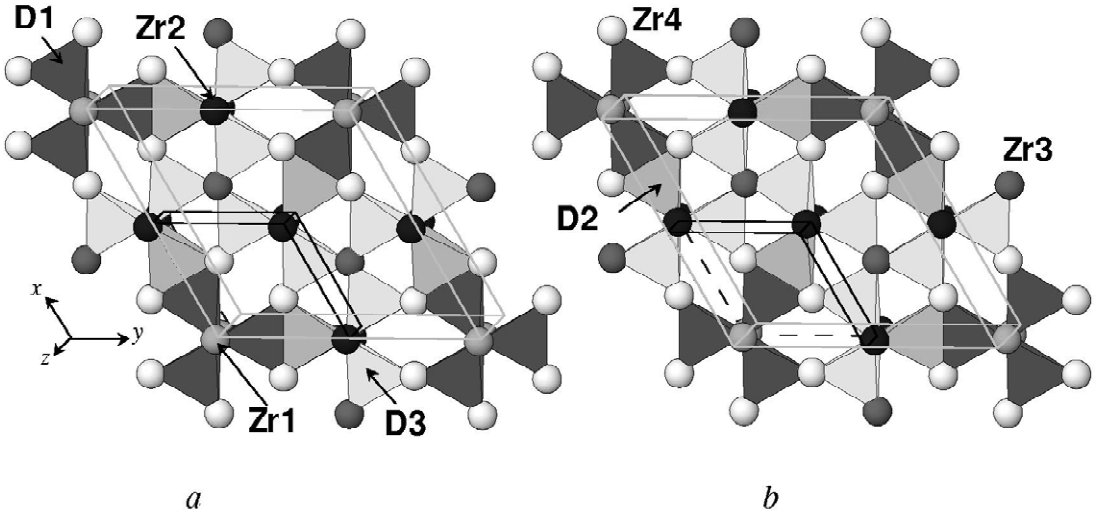

Fig. 3. Altering layers of the occupied Zr_4 interstices in the crystal structure of $Zr_4Al_3D_{2.68}$ viewed along [001] at $z=0$ (*a*) and $z=1/2$ (*b*). The borders of the original subcell and the superstructure cell are shown.

$Zr_4Al_3D_3$ hydrogen diffusion is not possible along [001] and proceeds via the two-dimensional diffusion paths located in the planes, which are perpendicular to the *c*-axis. The ordering of deuterium atoms within hydrogen sublattice eliminates short D . . . D separations, so the shortest distance between the occupied Zr_4 sites, 2.402 Å (D1 . . . D2), exceeds 2 Å. The shortest D–D distance between the neighbouring D layers is very long, 5.75 Å.

The occupancies of the three filled Zr_4 sites are slightly different, from 80.9 to 100%. Thus, the overall stoichiometry, $Zr_4Al_3D_{2.68}$, is smaller than the ideal value of $Zr_4Al_3D_{3.0}$. Since the metal sublattice is slightly deformed, the occupied Zr_4 sites are non-equivalent in size. Radii of the occupied interstices in the structure fall within the range 0.42 . . . 0.47 Å, which is lower than the size limit for the occupied interstices in the chemically related $Zr_2FeD_{5.0}$, $Zr_3FeD_{6.7}$ and $Zr_6FeAl_2D_{9.8}$, 0.48 . . . 0.53 Å [8,9]. Smaller size of the occupied interstices in $Zr_4Al_3D_{2.68}$ is caused by short Zr1 . . . Zr1 separations in the structure (2.740 Å), which even in the saturated hydride are 15% shorter than the doubled radius of Zr atom (3.204 Å). Radii of the empty interstices in this structure vary from 0.39 to 0.44 Å.

Since D atoms avoid filling interstices having Al in their surrounding, the shortest D . . . Al separation exceeds 3 Å.

3.3. Crystal structure of $Zr_3Al_2D_{2.26}$

The hydrogenation of Zr_3Al_2 intermetallic compound preserves its tetragonal symmetry and results in an anisotropic expansion of the unit cell ($\Delta a/a_0=-0.4\%$; $\Delta c/c_0=3.9\%$; $\Delta V/V_0=3.2\%$). The crystal structure data for this compound are given in Table 3. In $Zr_3Al_2D_{2.26}$ hydrogen atoms completely occupy tetrahedral interstices $8i_1Zr_4$. In addition to this site, H atoms enter $16k_2$ site inside the $Zr_1Zr_2Zr_3Al$ tetrahedron ($r=0.43$ Å). However, since D2 atoms are shifted from the ideal centre of the tetrahedral interstice away from Al atoms, it makes them coordinated by the $Zr_1Zr_2Zr_3$ triangle only. Such a shift increases Al–D2 distance to 2.082 Å and indicates nonbonding interaction between D2 and neighbouring Al atom. The occupied tetrahedral interstices form a spatial framework by sharing common vertices and/or edges. In hydrogen sublattice D1 atoms are separated from neighbouring D atoms by at least 2.407 Å (D1 . . . D2). D2 site is a split-position with the distance to the similar D2 site of 1.65 Å. Because of rather small, 6%, occupancy of this site, neighbouring D2 sites are presumably never simultaneously filled and such short D2 . . . D2 separations are avoided. Deuterium atoms are situated inside the columns formed from the $ZrZr_8$ cubes and form a 8-vertex coordination polyhedron around Zr1 (Fig. 4). The radius of the completely occupied Zr_4 tetrahedron, 0.51 Å, fits well with the earlier observed range of the radii for the significantly occupied interstices in the structures of Zr-based hydrides [8].

3.4. Thermal stability of deuterides

Thermal stability of the studied deuterides and Zr–D bonding characteristics can be related to the size of the occupied Zr_4 tetrahedra. Higher thermal stability of $Zr_3Al_2D_{2.26}$ (decomposition with the main desorption event at 600 °C) agrees well with the existence of large Zr_4 sites and contrasts to the behaviour of $Zr_4Al_3D_{2.68}$ containing 'contracted' Zr_4 tetrahedra and having weaker Zr–D bonds (desorption starts at much lower temperature of 400 °C).

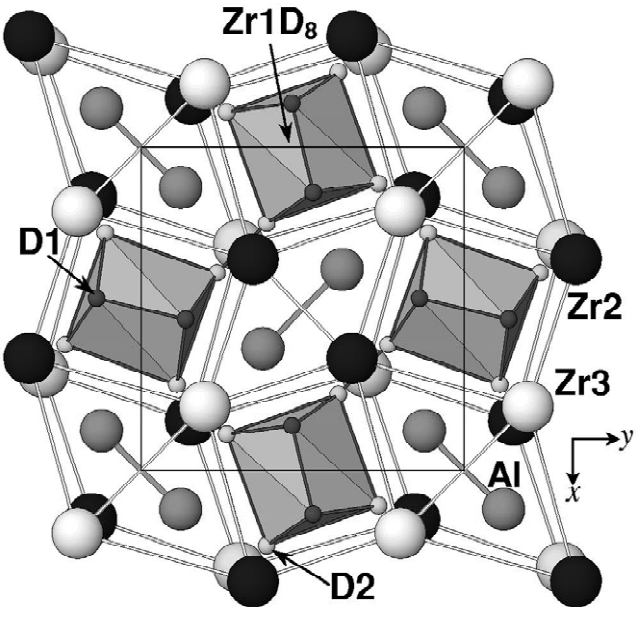

Fig. 4. The crystal structure of $Zr_3Al_2D_{2.26}$ viewed along [001]. Deuterium atoms form 8-vertexes polyhedra around Zr1 atoms and are located inside the columns built from the $Zr1Zr_8$ cubes. Al atoms form pairs and are coordinated by the side-connected trigonal prisms Zr_6.

Conclusions

H storage capacity of the chemically related Zr–Al intermetallics is influenced by the ratio of active (Zr) and non-active (Al) to the hydrogenation constituents. After reaching maximum possible occupation of the Zr-formed Zr_4 tetrahedra, hydrogen atoms enter less attractive and smaller in size Zr_3 triangular sites revealing the nonbonding interactions with the neighbouring Al-atoms. Filling of Zr_3 sites allows the hydrogenation capacity of $Zr_3Al_2D_{2.26}$ (0.45 at.D/at.M) to exceed that of $Zr_4Al_3D_{2.68}$ (0.38 at.D/at.M) and can be related to a more dense packing of the metal atoms in Zr_4Al_3, with shorter distances between Zr atoms compared to Zr_3Al_2.

Further studies of Al-containing intermetallics as H storage materials are important to find the ways of involving Al into the hydrogenation process thus approaching high H weight content (10 wt.%) of AlH_3.

Acknowledgements

The skilful assistance from the project team at the Swiss–Norwegian Beam Line, ESRF, is gratefully acknowledged.

References

[1] K.H.J. Buschow, P.C. Bouten, A.R. Miedema, Rep. Progr. Phys. 45 (1982) 937.
[2] N.J. Clarck, E. Wu, J. Less-Common Metals 142 (1988) 148.
[3] K.N. Semenenko, E.E. Fokina, V.N. Fokin, S.L. Troitskaya, V.V. Burnasheva, Izv. AN SSSR. Ser. Chem. (1980) 2634.
[4] T. Larsson, Y. Andersson, S. Rundqvist, R. Tellgren, N.J. Clark, E. Wu, Z. Phys. Chem. 179 (1993) 217.
[5] P. Villars, L.D. Calvert, Pearson's Handbook of Crystallographic Data for Intermetallic Phases, 2nd Edition, ASM International, Materials Park, OH, 1991.
[6] A.C. Larson, R.B. von Dreele, General Structure Analysis System (GSAS), LANSCE, MS-H 805 (1994).
[7] W.B. Pierson, The Crystal Chemistry and Physics of Metals and Alloys, Interscience, New York, 1972.
[8] V.A. Yartys, H. Fjellvåg, I.R. Harris, B.C. Hauback, A.B. Riabov, M.H. Sørby, I.Yu. Zavaliy, J. Alloys Comp. 293–295 (1999) 74.
[9] V.A. Yartys, Crystal chemistry of novel intermetallic hydrides, 8th European Conference on Solid State Chemistry, Oslo, Norway, July, 2001, I-6.